Dalton Transactions

Accepted Manuscript

ROYAL SOCIETY OF CHEMISTRY

www.rsc.org/dalton

Journal Name

RSCPublishing

ARTICLE

A heterotrimetallic Ir(III), Au(III) and Pt(II) complex incorporating cyclometallating bi- and tridentate ligands: simultaneous emission from different luminescent metal centres leads to broad-band light emission

Cite this: DOI: 10.1039/x0xx00000x

Received 00th January 2012,
Accepted 00th January 2012

DOI: 10.1039/x0xx00000x

www.rsc.org/

Rebeca Muñoz-Rodríguez,[a] Elena Buñuel,[a] Noelia Fuentes,[a] J. A. Gareth Williams,[b]* and Diego J. Cárdenas[a]*

Di- and tri-nuclear metal complexes incorporating gold(III), iridium(III) and platinum(II) units linked via a 1,3,5-triethynylbenzene core are reported, together with the corresponding mononuclear complexes as models. The gold(III) and platinum(II) units comprise tridentate, cyclometallating, C^N^C and N^N^C-coordinating ligands respectively, with the Ar-C≡C– directly bound to the metal at the fourth coordination site. The iridium moiety is an $Ir(ppy)_2(acac)$ unit bound to the triethynylbenzene through a phenyl substituent at the 3-position of the acac ligand. The multinuclear compounds are prepared using a modular synthetic strategy from the monometallic complexes. All of the compounds are luminescent in solution at room temperature, and their photophysical properties have been studied. The triplet excited state energies of the mononuclear complexes lie in the order Au > Ir > Pt. Consistent with this order, energy transfer from Au to Ir and from Au to Pt is observed, leading to quenching of the Au emission in the gold-containing multinuclear complexes. Energy transfer from Ir to Pt occurs at a rate that only partially quenches the Ir-based emission. As a result, the dinuclear Ir-Pt and trinuclear Au-Ir-Pt complexes display broad emission across most of the visible region of the spectrum.

Introduction

Luminescent complexes of second and third row d^6 and d^8 metal ions have attracted much attention due to their interesting optical properties. These complexes have been used to construct a variety of devices including organic light-emitting diodes (OLEDs),[1-4] chemical sensors,[5-7] bioimaging agents,[8] and nonlinear optical systems.[9-10] The large spin-orbit coupling constant of such metal ions, particularly those from the 3rd row, can lead to efficient phosphorescence from triplet states, even at room temperature, a process rarely possible in all-organic systems.[11] In OLEDs, this allows the otherwise wasted triplet states to be harvested, leading to 4-fold increases in device efficiency compared to fluorescent systems.[12] Meanwhile, in bioimaging, the longer lifetime of luminescence of such metal complexes (typically around a microsecond) allows time-resolved discrimination from background fluorescence (which occurs on the nanosecond timescale), with accompanying increases in sensitivity.[13]

White-light-emitting materials and devices have attracted much interest because of their potential applications in, for instance, solid-state lighting, full-color displays, and backlights.[14] The basic principle for generating white light from an OLED involves combining light output from multiple emission centres of the three primary colors (red, green, and blue).[15] One of the difficulties of such an approach is that energy-transfer between the dopants will tend to favour emission from the red emitter at the expense of the green and blue, essentially a "short-circuiting" of the system. This problem can be overcome by segregating the emitters into different layers, but this adds to device complexity and cost. Single compounds that emit efficiently across the visible region, preferably from triplet states, are therefore of much interest.[16]

Cyclometallating ligands have proved to be particularly successful in generating luminescent complexes, owing to their strong ligand fields which ensure that potentially deactivating d-d states are destabilised.[17] Cyclometallated iridium(III) complexes are robust, easy to produce, synthetically versatile, photochemically and thermally stable and display attractive photophysical properties.[18] Indeed, they already feature as green and red emitters in the OLED displays of mass-produced devices. Meanwhile, cyclometallated platinum(II) complexes

are attracting increasing interest, partly due to their potential for white light generation through excimer formation, a process not possible for the pseudo-octahedral complexes of the d^6 iridium(III) ion.[16] For platinum(II), the use of tridentate cyclometallating ligands, such as phenylbipyridine or dipyridylbenzene, can be advantageous over bidentate ligands, owing to the greater rigidity of their complexes.[19,20] In contrast to Ir(III) and Pt(II), there are far fewer examples of Au(III) complexes that display appreciable luminescence at room temperature. The lack of luminescence from many Au(III) complexes may be due to the presence of higher-lying but thermally accessible deactivating states (e.g. d-d or LMCT states), and/or to the lower energy of filled metal orbitals in Au(III) complexes compared to Pt(II) analogues.[21] This latter feature results in lower metal character in the excited state and hence to less efficient spin-orbit coupling pathways and low radiative rate constants. The use of strong-field cyclometallating ligands and/or σ-donating alkynyl or N-heterocylic carbenes can alleviate both issues indeed,[22] quite intense luminescence has recently been reported for a group of cyclometallated Au(III) complexes with 2-phenylpyridine ligands and alkynyl co-ligands.[22d]

As far as *multinuclear* cyclometallated complexes comprising these elements are concerned, homo-dinuclear platinum(II) complexes have been investigated, often with a view to exploring intramolecular excimer/aggregate formation.[19,23,24] Energy transfer between covalently-linked iridium centres has been studied in supramolecular Ir_nRu assemblies (n = 3 or 7).[25] In both of these cases, the properties of the individual metal-containing units are largely retained, and the observed phenomena involve face-to-face interactions or energy transfer processes between the discrete units respectively. In contrast, when the metal ions are closer together and bound to a common heterocyclic ring, the properties of the resulting multimetallic assembly differ more profoundly from the mononuclear analogues, with a significant red-shift of the absorption and emission.[26] There are, however, very few heterometallic compounds featuring combinations of Au(III), Pt(II) and Ir(III). Previously, we studied a rigid gold-platinum dinuclear complex constructed on a xanthene scaffold, in which rapid Au to Pt energy transfer was observed.[24] Trinuclear complexes incorporating Ir(III) and Os(II) units assembled around a triptycene or spirobifluorene core, and related compounds with Pt(II), Ru(II) and Os(II) units linked through a central truxene moiety, have been reported in a series of studies by Ziessel, Ventura and co-workers.[27] The metal units in these supramolecular compounds essentially retain the properties of the individual complexes, and energy transfer is observed between them. Kozhenikov *et al.* have explored a Pt_2Ir trimer, which behaves as a single chromophore whose excited-state properties are very different from those of the constituent units.[28]

In this work, we report on the synthesis and luminescence properties of a unique heterotrimetallic complex **7** (Figure 1) featuring cyclometallated Au(III), Ir(III) and Pt(II) units linked through a 1,3,5-triethynylbenzene core. The Au(C^N^C), $Ir(N^C)_2$ and Pt(N^N^C) units selected were chosen on the basis that the analogous mononuclear complexes display blue/green, green and orange/red luminescence respectively. The limited conjugation between *meta* related postions within a benzene ring might be expected to limit the rate of through-bond energy transfer procesess between the metal centres, whilst analysis of through-space processes may be aided by the rigidity of the system, which ensures that the units are kept at a constant separation within the molecule. We were intrigued to explore whether the compound would show multiple emissions from the metal units, to give broad-band emission, or whether fast energy-transfer to the Pt(II) unit would lead to emission from this centre only. Related monometallic and dimetallic (Au-Pt, Au-Ir, Ir-Pt) complexes incorporating the triethynyl benzene unit are also described, whose properties are important in allowing those of the trinuclear complex to be rationalised.

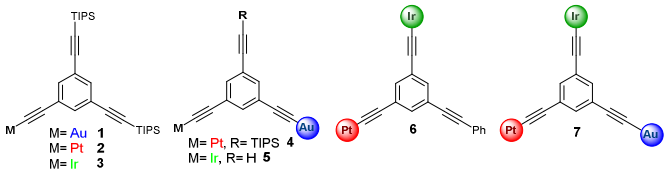

Figure 1. Schematic structures of the mono- and hetero-nuclear Pt(II), Au(III) and Ir(III) complexes. The full coordination spheres of the metal ions are shown in Schemes 1 to 4

Results and discussion

Synthesis

The three mononuclear complexes incorporate the same central framework, in which a 1,3,5-triethynyl benzene carries tri-isopropylsilyl (TIPS) protecting groups at the termini of two of the three alkynyl units and the third is linked to the metallic unit (Scheme 1). For the gold and platinum complexes, the Ar-C≡C- group is directly coordinated to the metal ion, whereas for the iridium complex, it is linked to a coordinating acac unit through an interposed phenyl group. The synthetic route (Scheme 1) involves incorporation of metal complexes on doubly protected alkyne **8**.[29] Thus, treatment of **8** with the previously prepared metal complexes **9** or **10**[24] in the presence of CuI and Et_3N, gave the desired mononuclear Au(III) and Pt(II) complexes **1** and **2** respectively. The preparation of the Ir(III) complex **3** was carried out by Pd/Cu-catalysed Sonogashira coupling with a bis-cyclometallated iridium complex carrying a phenyliodo-substituted acac ligand, **11**. A similar procedure has been used recently by others to prepare iridium complexes featuring pendent aryl substituents attached to the acac via a C≡C linker.[30]

The preparation of the dinuclear complexes could not be carried out from mononuclear derivatives **1-3**, since selective deprotection of just one of the TIPS groups could not be achieved.

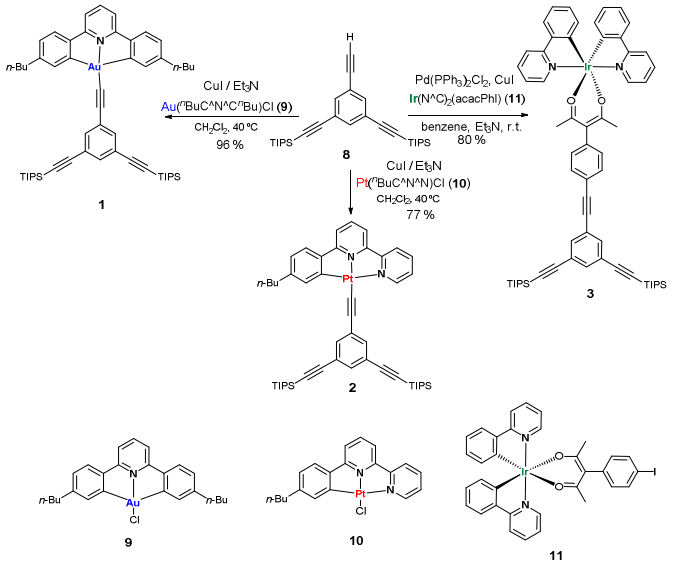

Scheme 1. Synthesis of mononuclear compounds

Instead, we selected a different mononuclear Au(III) complex, namely **13**, as a precursor to dinuclear complexes. It incorporates one terminal alkyne and one TIPS-protected alkyne. Its synthesis is shown in Scheme 2 and involves dialkyne **12**,[31] as starting material. Treatment of **12** with the bis-cyclometallated gold precursor **9** gave the Au(III) complex **13**, which was then reacted with the cyclometallated platinum precursor **10** under similar conditions to give the heterodinuclear Au-Pt complex **4**.

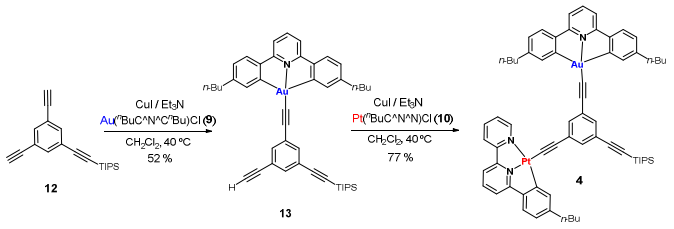

Scheme 2. Synthesis of the heterodinuclear Au-Pt compound **4**

Unfortunately, the synthesis of heterodinuclear compounds containing the Ir(III) unit could not be carried out from **13**, because **13** undergoes dimerization under the reaction conditions. Therefore, a different strategy was devised, using a mononuclear Ir(III) complex **14** that carries two terminal alkynes, and is obtained by desilylation of **3** with $(n\text{-Bu})_4$NF (Scheme 3).

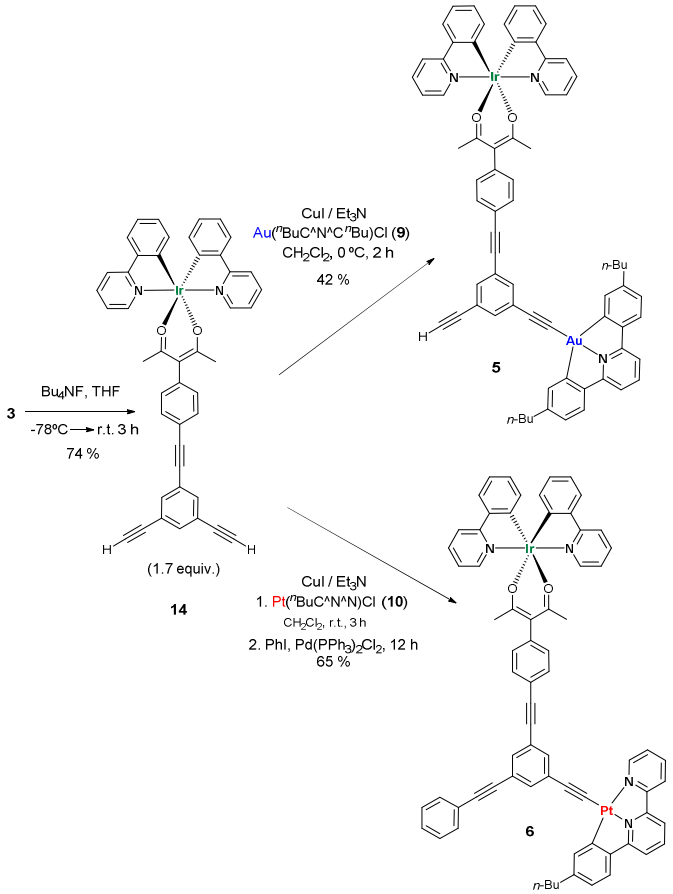

Scheme 3. Synthesis of the heterodinuclear compounds **5** (Au-Ir) and **6** (Ir-Pt)

Treatment of **14** with the Au precursor complex **9** (0.59 equiv) in the presence of CuI and Et_3N gave the dinuclear Au-Ir complex **5**. The same route was used to obtain a dinuclear Ir-Pt complex, but the initially formed product proved difficult to isolate and purify. Consequently, an excess of iodobenzene and catalytic $Pd(PPh_3)_2Cl_2$ were added at the end of the reaction in order to arylate the free alkyne, to give the Ir-Pt complex **6**, which could be isolated and purified more readily.

Finally, the heterotrinuclear Au-Ir-Pt complex **7** was synthesized from **5** by treatment with the precursor Pt complex **10** in the presence of CuI and Et_3N, as shown in Scheme 4.

Photophysical properties

Photophysical data for the complexes **1**–**7** are compiled in Tables 1 and 2, and selected absorption and photoluminescence spectra are shown in Figures 2–5.

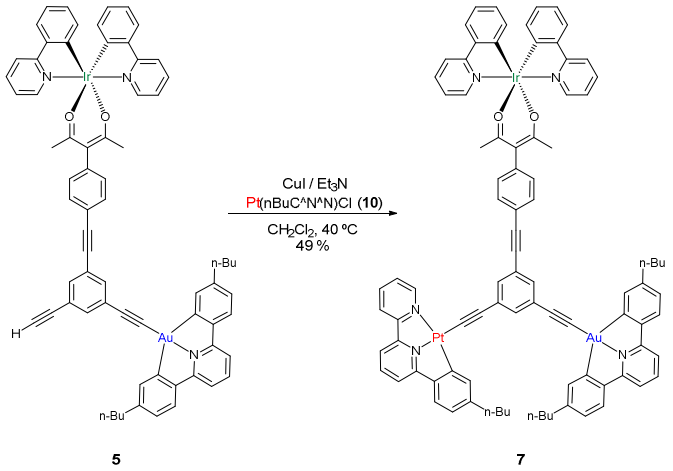

Scheme 4. Synthesis of the heterotrinuclear Au-Ir-Pt compound **7** from dinuclear complex **5**

(i) Mononuclear complexes.

We shall first consider the mononuclear complexes **1**–**3**. The absorption spectrum of the mononuclear Au(III) complex **1** (Fig. 2a) displays a vibronically structured band around 400 nm, typical of cyclometallated Au(III) complexes with C^N^C-coordinating ligands, corresponding to predominantly spin-allowed intraligand (^{1}IL) transitions with a small participation of the metal.[32] This complex emits weakly in solution at room temperature, displaying a structured band, λ_{0-0} = 484 nm (Fig. 2a), assigned to the ^{3}IL transition with a small participation of the metal; Φ_{lum} = 4.4 x 10^{-4}, τ = 120 ns. Assuming, nevertheless, that the triplet state is formed with approximately unitary efficiency, the radiative k_r and non-radiative Σk_{nr} decay constants can be estimated on the basis that $k_r = \Phi_{lum}/\tau$ and $\Sigma k_{nr} = \tau^{-1} - k_r$. The rather small value of k_r of 3700 s^{-1} thus obtained is consistent with the relatively small participation of the metal in the excited state, limiting the exent to which it can promote phosphorescence from the triplet state and allow it to compete with non-radiative decay. In a frozen glass at 77 K, under which conditions the non-radiative decay processes are inhibited, the lifetime increases greatly to 274 μs, a long value that is again indicative of a small metal contribution.

The absorption and emission properties of the mononuclear Pt(II) complex **2** are typical of Pt(II) complexes with N^N^C-coordinating ligands based on phenylbipyridine (phbpy). The absorption spectrum features moderately intense bands in the 400–500 nm region associated with charge-transfer transitions, and the complex displays a structureless emission band at room temperature, λ_{max} = 586 nm, Φ_{lum} = 7.0 x 10^{-2}, τ = 570 ns (Fig. 2b). These values are similar to those reported previously for Pt(phbpy)(C≡C-Ph).[19b]

Finally, the mononuclear Ir(III) complex **3** displays an absorption spectrum characteristic of cyclometallated Ir(III) complexes with ppy ligands, of the type Ir(*N^C*)$_2$(*O^O*), including a set of bands that extend into the visible region corresponding to metal-to-ligand charge-transfer transitions.[33]

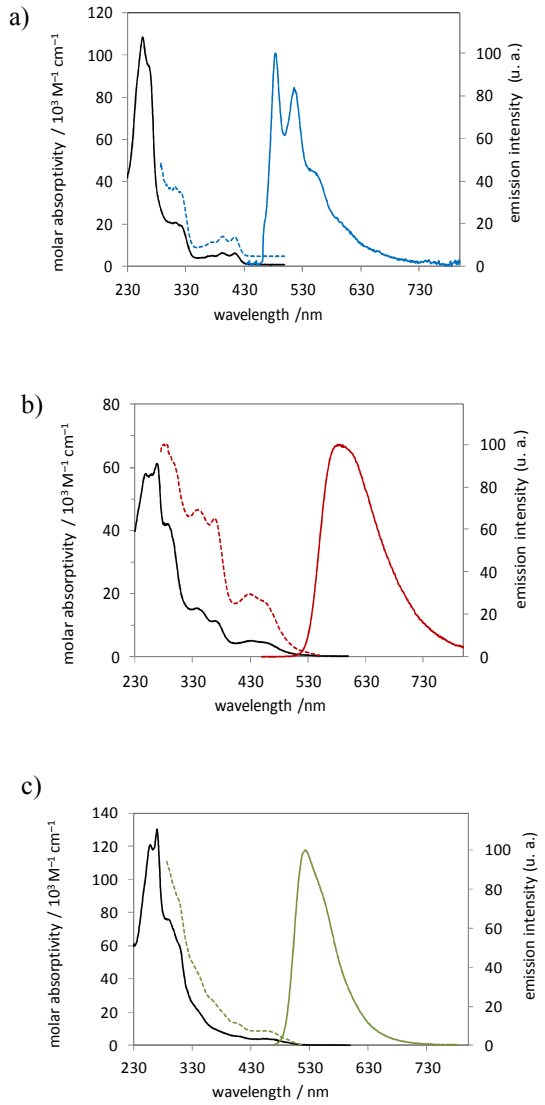

Figure 2. Absorption spectra (black solid lines), excitation (dashed lines) and emission (coloured solid lines) spectra of Au complex **1** (a), Pt complex **2** (b) and Ir complex **3** (c) in deoxygenated CH_2Cl_2 solution at 298 K

This complex emits brightly in solution at room temperature, with a structureless emission band (Fig. 2c) emanating from the ^{3}MLCT state; λ_{max} = 523 nm, Φ_{lum} = 0.31, τ = 880 ns. These data are similar to those of the structurally similar complex of the form (ppy)$_2$Ir(acac)C$_6$H$_4$(C≡C-tolyl), referred to above.[30]

Figure 3a shows the emission spectra of the three mononuclear complexes on the same scale for convenience, together with the spectra at 77 K. Owing to the broadness of the Ir(III) and Pt(II) spectra, which do not show a clear 0–0 band at room temperature, the 77 K data have been used to generate an energy level diagram for the lowest triplet states of the

complexes (Fig 3b). It is clear that energy transfer from the Au to the Ir and Pt unit, and from the Ir to the Pt unit, could be anticipated in the multinuclear systems, which are discussed in the following sections.

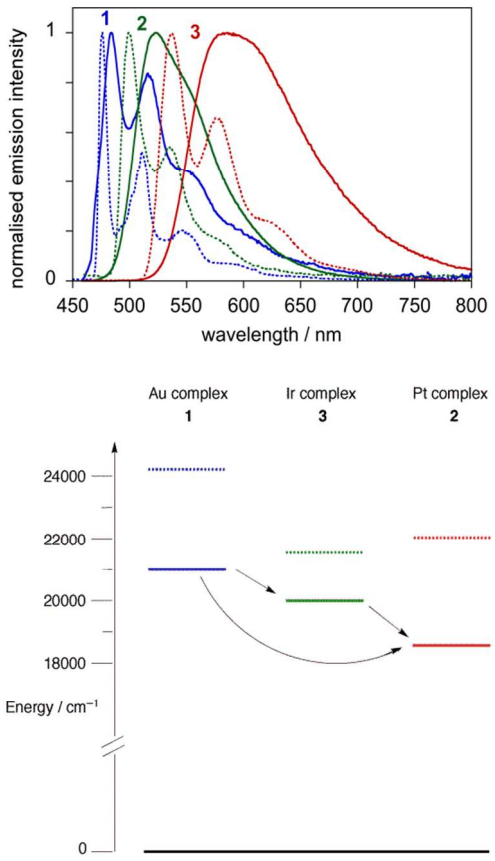

Figure 3. (a) Top: Normalised emission spectra of 1 (blue), 2 (green) and 3 (red) in deoxygenated CH_2Cl_2 solution at 298 K (solid lines) and in diethyl ether / isopentane / ethanol (2:2:1 v/v) at 77 K (dotted lines). (b) Bottom: Energy level diagram showing the approximate energies of the T_1 excited states (solid lines, estimated from the 77 K emission spectra) and the S_1 excited states (dotted lines, estimated on the basis of the lowest-energy intense – *i.e.* spin-allowed – bands in the absorption spectra). The arrows show the expected directions of energy transfer.

(ii) Dinuclear complexes.

The absorption spectrum of the dinuclear Au-Pt complex **4** displays features characteristic of both the mononuclear Au (**1**) and Pt (**2**) complexes. Indeed, the experimental spectrum is very similar to that simulated by addition of the spectra of **1** and **2** (see Supporting Information), indicative of minimal conjugation and limited ground-state communication between the metal centres. On the other hand, excitation of **4** at room temperature results in a single emission band, similar in energy and profile to that displayed by the mononuclear Pt complex **2** (Fig. 4a), irrespective of the excitation wavelength employed. The excitation spectrum incorporates the structured bands in the 360–430 nm region that are characteristic of the Au complex. These data suggest that excitation of the Au unit is followed by rapid energy transfer to the Pt unit, at a rate that is sufficiently fast that emission from the Au unit becomes undectable under these conditions. The rate of the energy transfer process is considered in more detail in section (iv) below. The luminescence quantum yield is of a similar magnitude, though somewhat reduced, in **4** compared to the mononuclear Pt complex **2**. Normally, if fast energy transfer occurs, Φ should be determined largely by the emitting unit and a similar value expected. Given the rather large uncertainty on quantum yield measurements (±20%), there is a danger in over-interpreting the small difference. It is possible that the excited state becomes somewhat more extended in **4** compared to **2** through the effect of the Au ion, such that the net Pt character in the excited state is slightly diminished and hence the radiative rate constant k_r reduced, as observed (Table 2). At 77 K, for $\lambda_{ex} < 430$ nm, a very weak band assignable to residual Au-based emission is detectable (see Supporting Information Fig 5). For longer excitation wavelengths, no Au component to the emission is observed, consistent with the fact that, of the mononuclear Au and Pt complexes **1** and **2**, only the Pt complex **2** absorbs at such wavelengths.

Similar observations are made for the dinuclear Au-Ir complex **5**. Its absorption spectrum is again similar to that simulated by addition of the spectra of the two constituent mononuclear complexes (see Supporting Information). The emission spectrum at room temperature shows a single band similar in energy and profile to that of **3** (Fig. 4b), and the luminescence lifetime is very similar to the value for **3** (Table 2). These data again suggest that those photons absorbed by the Au unit are transferred to the Ir unit, at a rate sufficient to render the weak Au emission undetectable. The quantum yield is of the same order of magnitude but somewhat reduced compared to **3**, apparently due to a lower k_r value although it is difficult to rationalise such an effect in this instance. At 77 K for $\lambda_{ex} < 430$ nm, a very weak band assignable to Au emission is detectable (see Supporting Information Fig 6).

The absorption spectrum of the dinuclear Ir-Pt complex **6** also matches well with that simulated by addition of the spectra of its constituent mononuclear complexes **2** and **3** (see Supporting Information). However, in this case, the emission spectrum at room temperature clearly shows two components: a broad structureless band with $\lambda_{max} = 577$ nm accompanied by a weaker yet distinct shoulder at 520 nm (Fig. 4c). They can be attributed to emission from the Pt and Ir moieties respectively. The emission of the Pt unit can be monitored independently of the Ir unit since the Pt emission extends out to longer wavelengths (Fig. 2). For example, at 700 nm, the luminescence decay follows monoexponential kinetics giving a lifetime of 570 ns, the same as that recorded for Pt complex **2**. The emission of the Ir unit cannot be monitored independently of the Pt unit, since it overlaps with the emission of the Pt unit. The luminescence decay monitored in the shorter-wavelength region of the spectrum (e.g. λ_{em} = 520 nm) displays biexponential kinetics, with components of 560 ns and 25 ns

corresponding to the Pt and Ir units respectively (Table 2). It may be noted that the lifetime associated with the Ir emission band is much shorter than that of the mononuclear Ir complex **3** (880 ns), indicative of energy transfer from the Ir unit to the Pt component, but at a rate {see section (iv) below} that is not sufficient to completely quench the emission from the Ir component. The relative contribution of the shoulder due to the Ir unit in the emission spectrum is essentially independent of the excitation wavelength. At 77K, the high-energy band shifts slightly to the blue, whilst the main lower-energy band becomes vibrationally resolved showing three main components (see Supporting Information Fig 7). This trend upon cooling is fully consistent with the spectra of the two mononuclear units at 77 K (Fig 3a, Table 2).

At 77K, the high-energy band shifts slightly to the blue, whilst the main lower-energy band becomes vibrationally resolved showing three main components (see Supporting Information Fig 7). This trend upon cooling is fully consistent with the spectra of the two mononuclear units at 77 K (Fig 3a, Table 2).

Table 1 UV-visible absorption data for the complexes **1**–**7**[a]

Complex	Absorption λ_{max} / nm (ε / $M^{-1}cm^{-1}$)
1 **Au**	256 (108500), 262sh (98300), 312 (20600), 320(19400), 367sh (4590), 393 (6330), 413 (6140)
2 **Pt**	268 (61200), 280 (42500), 338 (15400), 367 (11300), 430 (5050), 462sh (4160)
3 **Ir**	259 (122000), 270(131400), 287 (76700),306sh (63000), 339 (22400), 407 (5560), 458 (4920)
4 **Au-Pt**	261 (93400), 321 (29900), 372 (15300), 415 (9400), 443 (5150)
5 **Au-Ir**	262 (108400), 306sh (62300), 364sh (13600), 381 (11000), 411 (9020), 456 (3390)
6 **Ir-Pt**	288 (124500), 337 (47500), 368sh (23800), 408sh (11100), 455 (9110)
7 **Au-Ir-Pt**	264 (148900), 342sh (37700), 368 (24900), 413 (14000), 450 (7820)

[a] Absorption spectra were recorded for solutions of concentrations in the range 2×10^{-5} to 1×10^{-4} M, over which the absorbance was confirmed to vary linearly with concentration.

However, under these conditions, only one lifetime can be resolved, of 6 μs, with no significant dependence on the wavelength at which the emission is monitored. The lifetime at 500 nm is not significantly shorter than at longer wavelengths, as might have been expected on the basis of the behaviour at room temperature. It is notable, however, that at 77 K the Pt and Ir mononuclear complexes (2 and 3) both have lifetimes of around 5 or 6 μs. Apparently, then, the Ir→Pt energy transfer rate in 6 is slowed down under these conditions, and the two units behave essentially independently.

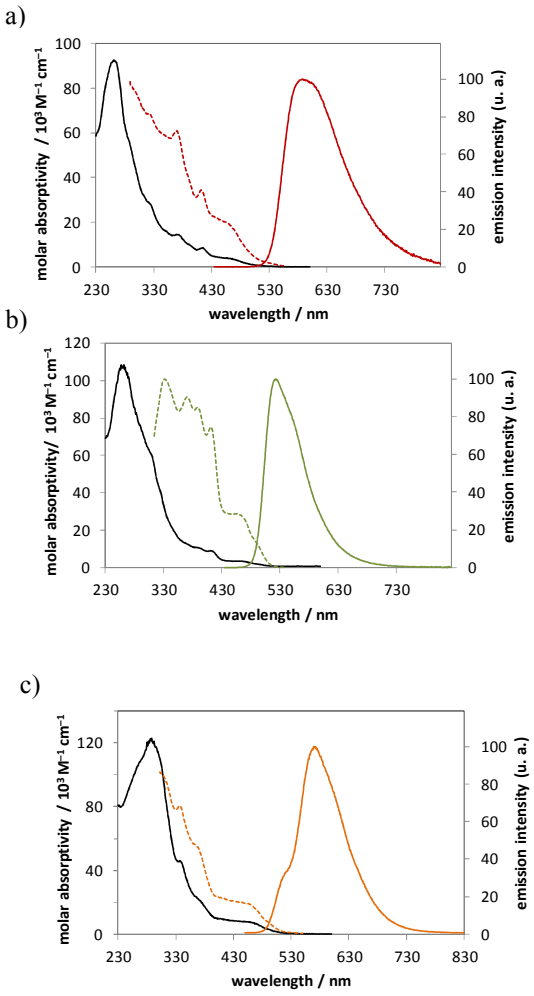

Figure 4. Absorption spectrum (black solid line), excitation (dashed line) and emission (colour solid line) spectra of dinuclear complexes Au-Pt **4** (Figure a), Au-Ir **5** (Figure b) and Ir-Pt **6** (Figure c) in CH_2Cl_2 at 298 K

(iii) Trinuclear complex

The absorption spectrum of the trinuclear complex **7** is similar to that simulated by addition of the spectra of the three mononuclear Au, Pt and Ir complexes **1**, **2** and **3** (see Supporting Information). This observation is consistent with the behaviour of the binuclear complexes, and is indicative of rather minimal ground-state interactions between the three units. The emission spectrum of **7** resembles that of **6** (dinuclear Ir-Pt derivative) showing two components: a broad band centred at 577 nm attributable to emission from the Pt unit, and a weaker, high-energy shoulder which can be assigned to residual Ir emission (Fig. 5a).

No higher-energy emission attributable to the Au component is detectable. The decay in the shorter-wavelength region (λ_{em} = 520 nm was selected) displays biexponential kinetics, with components of 670 ns and 42 ns respectively, attibutable to emission from the Pt and Ir units. The data support the expectation, based on the behaviour of the dinuclear complexes, that energy absorbed by the Au unit will be transferred to the Pt unit and/or to the Ir unit, and that the excited state of the Ir unit will be predominantly deactivated by energy transfer to the Pt unit, which has the lowest excited state energy (Fig. 3). As in **6**, the rate of this energy transfer is apparently not fast enough to lead to the complete disappearance of the emission from the Ir unit. Again, the proportion of Ir-based emission in the spectrum is approximately independent of the excitation wavelength employed.

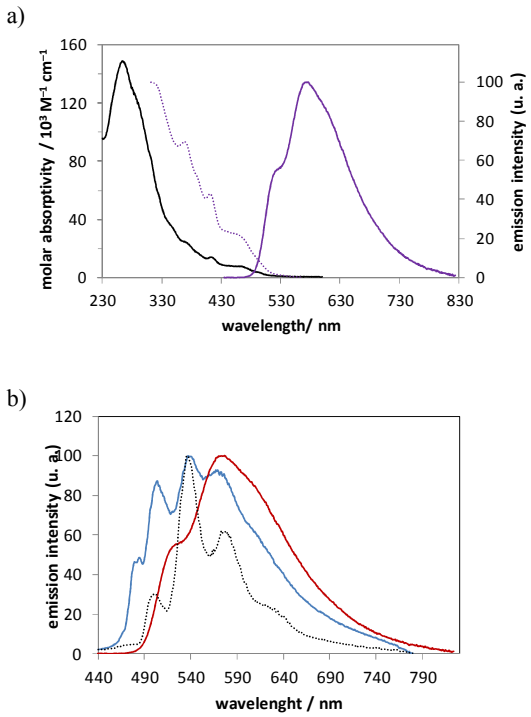

Figure 5. a) Absorption spectrum (black solid line), excitation (dashed line, λ_{em} = 650 nm) and emission (colour solid line, λ_{ex} = 415 nm) spectra of **7** in CH_2Cl_2 at 298 K. b) Emission spectra of **7** in CH_2Cl_2 at 298 K (red line), and of **7** and **6** at 77 K in diethyl ether / isopentane / ethanol (2:2:1 v/v) (solid blue and black dotted lines respectively); λ_{ex} = 415 nm in each case.

At 77 K, for $\lambda_{ex} < 430$ nm, the emission spectrum displays four components (Fig. 5b). Based on the spectra of the mononuclear and dinuclear complexes, the bands can reasonably be assigned as follows. The two lowest-energy bands (λ = 537 and 567 nm) are due to emission from the Pt unit with vibrational components as observed in Fig. 3a. The band at 504 nm can be attributed to emission from the Ir component and that at 483 nm to the Au unit. A lifetime of 200 μs is registered at 480 nm, whilst a much shorter value of around 5.6 μs is recorded at 535 nm, and similarly at 500 nm. The long lifetime of the high-energy band is consistent with the behaviour of the Au component at 77 K, and with the observations made for the Au-Pt and Au-Ir dinuclear complexes. On the other hand, the fact that the Ir-based emission cannot be resolved kinetically from the Pt emission is consistent with the results for the Ir-Pt complex at 77 K, the two units having similar lifetimes under these conditions.

(iv) Energy transfer.

The observation of dual emission in **6** and in **7**, with bands attributable to the Ir and Pt components appearing simultaneously, allows the rate of energy transfer to be considered in more detail. We will consider the Ir-Pt dinuclear complex **6**. The rate of energy transfer, k^{ET}, from Ir to Pt can be estimated on the basis of the extent to which the lifetime of the Ir emission component is shortened compared to its value in the mononuclear Ir complex **3**, as in equation [1]:

$$k^{ET} = \tau_{(\mathbf{Ir}-Pt)}^{-1} - \tau_{Ir}^{-1} \qquad [1]$$

where $\tau_{(\mathbf{Ir}-Pt)}$ is the lifetime of the short component of the emission detected at 520 nm in **6**, and τ_{Ir} is the luminescence lifetime of **3**. This approach assumes that, apart from the introduction of energy transfer, the radiative and non-radiative decay processes open to the Ir unit are the same in **6** as in **3**. Although this assumption is unlikely to be strictly correct, it is probably valid to a first approximation. It gives a value of $k^{ET} = 4 \times 10^7$ s^{-1}.

An estimate of the rate of energy transfer through the Förster (through-space dipole–dipole) mechanism can be made, based on the absorption and emission properties of the mononuclear Pt and Ir complexes respectively. The Förster radius R_0 is given by equation [2]:

$$R_0^6 = 8.79 \times 10^{23} (\kappa^2 n^{-4} Q_D J(\lambda)) \qquad [2]$$

where Q_D is the quantum yield of the donor (the Ir unit), n is the refractive index (1.44 for CH_2Cl_2), and κ^2 is factor that takes into account the orientational dependence of the dipoles of donor and acceptor; a value of 2/3 applies to random averaging in intermolecular energy transfer, and will be used here.[34] The overlap integral $J(\lambda)$ is given by equation [3]:

$$J(\lambda) = \int_0^\infty F_D(\lambda)\varepsilon_A(\lambda)\lambda^4 d\lambda \qquad [3]$$

Table 2 Photophysical data for the mono-, di- and tri-nuclear complexes in deoxygenated CH_2Cl_2 at 298 K, except where indicated otherwise.

Complex	Emission λ_{max} / nm	τ / ns[a]	Φ_{lum}[b] x 10^2	k_r[c] / 10^3 s^{-1}	$\sum k_{nr}$[c] / 10^5 s^{-1}	Emission at 77 K[d] λ_{max}/nm	τ / μs[a]
1	484, 516,	120	0.044[e]	3.7	83	476,511, 546, 583	274
Au	555, 591sh						
2	586	570	7.0[f]	123	16	537, 575, 623, 683	5.8
Pt							
3	523	880	31[g]	354	7.9	499, 534, 576	5.0
Ir							
4	588	520	4.5[e]	86	18	477, 537, 577, 628	208 @478 nm
Au-Pt							6.3 @535 nm
5	523	860	14[e]	163	10	478, 500, 536, 680	211 @ 475 nm
Au-Ir							5.6 @500 nm
6	520sh, 577	570 @700 nm	5.1[f]	91	17	500, 536, 573, 625	6.0 @535 nm
Ir-Pt		τ_1 = 560, τ_2 = 25 @ 520 nm					
7	520sh, 577	580 @ 700 nm	7.2[e]	107	14	483, 504, 537, 567	200 @480 nm
Au-Ir-Pt		τ_1=670, τ_2 = 42 @520 nm					5.6 @535 nm

[a] λ_{ex} = 374 nm. The symbol @ indicates the emission wavelength (λ_{em}) at which the lifetime was measured; when no λ_{em} is indicated, the lifetime was found to be invariant (within the error) across the spectrum. [b] Quantum yield measured using $Ru(bpy)_3Cl_2$ in water as the standard. The concentrations of solutions were such that the optical density at the excitation wavelength employed was 0.1 or less. [c] k_r and Σk_{nr} are the radiative and non-radiative decay rate constants, estimated by assuming that the emissive state is formed with unitary efficiency, such that $k_r = \Phi_{lum} / \tau$ and $\Sigma k_{nr} = \tau^{-1} - k_r$. [d] Data at 77 K recorded in diethyl ether / isopentane / ethanol (2:2:1 by volume). [e] λ_{ex} = 415 nm. [f] λ_{ex} = 430 nm. [g] λ_{ex} = 460 nm.

where $F_D(\lambda)$ is the corrected emission spectrum of the energy donor (Ir complex **3**) with its integrated area normalised to unity, and $\varepsilon_A(\lambda)$ is the molar absorptivity of the acceptor unit (Pt complex **2**), with λ being the wavelength in cm. The overlap integral so calculated has a value of 2.13×10^{-15} $M^{-1}cm^3$, from which a Förster radius of 21.4 Å is obtained. From a simple molecular model, the distance, *r*, between the Pt and Ir metal centres in **6** is measured to be around 18.4 Å. Using this value in conjunction with the Förster radius, the rate of Förster energy transfer is calculated through equation [4], where τ_D is the lifetime of the Ir complex **3**.

$$k^{ET} = \frac{1}{\tau_D}\left(\frac{R_0}{r}\right)^6 \qquad [4]$$

A value of $k^{ET} = 2.8 \times 10^6$ s^{-1} is obtained. Although such a value would certainly introduce a significant deactivation of the iridium-based excited state, being of a similar magnitude to that of the luminescence decay rate constant of **3** (= 1.1×10^6 s^{-1}), it is significantly less than the k^{ET} value of 4×10^7 s^{-1} estimated above based on the change in the Ir lifetime. A significant Dexter contribution to the energy transfer rate is therefore highly likely, through the conjugated π system of the C≡C bonds and the central aryl ring. It may be noted that similar conclusions regarding the importance of triplet-triplet Dexter energy transfer have been reported in other recent studies of multimetallic systems incorporating triplet-emitting metal centres, such as Ru(II), Os(II) and Ir(III), assembled around cores which do not facilitate good conjugation in the ground state.[26]

The absence of detectable Au emission makes it difficult to determine experimental Au→Pt and Au→Ir energy transfer rate constants for **4** and **5** respectively. Förster radii of 8.35 Å and 8.45 Å respectively are calculated using equations [2] and [3], which – in conjunction with intermetallic distances, *r*, of 10.5 Å and 18.4 Å respectively – yield k^{ET} values of 2.1×10^{-6} s^{-1} and 7.8×10^{-4} s^{-1}. Again, these values are probably too small to account for the absence of detectable emission from the Au unit, although it must be noted that the quantum yield of the mononuclear Au complex **1** is two orders of magnitude lower than for the Pt and Ir analogues and for the multinuclear compounds, and so some residual Au emission in **4**, **5** and **7** could simply be obscured by the much higher intensity associated with the other metal centres.

Experimental

General information: NMR spectra were recorded on Bruker AC-300 MHz spectrometer. Chemical shifts are given in ppm. The spectra were calibrated to the residual ^1H and ^{13}C signals of the solvents. Multiplicities are abbreviated as follows: singlet (s), doublet (d), triplet (t), double triplet (dt), triple doublet (td), double double doblet (ddd) and multiplet (m). Absorption spectra were measured on a Biotek Instruments XS spectrometer, using quartz cuvettes of 1 cm pathlength. Steady-state luminescence spectra were measured using a Jobin Yvon FluoroMax-2 spectrofluorimeter, fitted with a red-sensitive Hamamatsu R928 photomultiplier tube; the spectra shown are corrected for the wavelength dependence of the detector, and the

quoted emission maxima refer to the values after correction. High-resolution mass spectrometry was performed on a QSTAR (Applied Biosystems) for ESI and ULTRAFLEX III (MALDI-TOF) (Bruker) for MALDI.

Synthesis of compounds 1-7:

Compound 1: A Schlenk was charged with **9** (72 mg, 0.125 mmol), 10 (87 mg, 0.188 mmol), Et_3N (0.6 mL) and CuI (6 mg, 0.029 mmol), followed by addition of anhydrous CH_2Cl_2 (10 mL). Then Ar was bubbled into the mixture for 3 min, the mixture was stirred at 40 ºC for 24 hours and finally concentrated in vacuo. The crude produced was purified by flash column chromatography on silica gel with hexane-CH_2Cl_2 (3:1) as eluent to give **1** (120 mg, 96%) as a yellow solid. ^{1}H NMR (300 MHz, $CDCl_3$): δ = 7.84 (d, *J* = 1.4 Hz, 2H), 7.76 (t, *J* = 8.0 Hz, 1H), 7.69-7.65 (m, 2H), 7.49-7.46 (m, 1H), 7.42 (d, *J* = 7.9 Hz, 2H), 7.34 (d, *J* = 8.0 Hz, 2H), 7.03 (dd, *J* = 7.9, 1.4 Hz, 2H), 2.68-2.58 (m, 4H), 1.73-1.56 (m, 4H), 1.47-1.31 (m, 4H), 1.15 (s, 42H), 0.94 (t, *J* = 7.3 Hz, 6H). ^{13}C NMR (75 MHz, $CDCl_3$, DEPT 135): δ = 166.9 (C), 165.2 (C), 147.6 (C), 146.6 (C), 142.1 (CH), 136.9 (CH), 135.3 (CH), 133.3 (CH), 127.4 (C), 126.9 (CH), 125.2 (CH), 123.8 (C), 116.0 (CH), 106.1 (C), 99.8 (C), 94.3 (C), 91.4 (C), 36.2 (CH2), 33.5 (CH_2), 22.6 (CH_2), 18.8 (CH_3), 14.1 (CH_3), 11.5 (CH). HRMS MALDI: Calcd for $C_{55}H_{73}AuNSi_2$ $[M+H]^+$ 1000.4945; found 1000.4929.

Compound 2: Anhydrous CH_2Cl_2 (7 mL) was added a Schlenk charged with **10** (42 mg, 0.082 mmol), **8** (57 mg, 0.123 mmol), Et_3N (0.4 mL) and CuI (4 mg, 0.019 mmol). Then Ar was bubbled into the mixture for 3 min and the mixture was stirred at 40 ºC for 48 h. The resulting mixture was then concentrated under reduced pressure and was purified by flash column chromatography on neutral Al_2O_3 with CH_2Cl_2 as eluent to give **2** (60 mg, 77%) as an orange solid. ^{1}H NMR (300 MHz, CD_2Cl_2): δ = 9.09 (d, *J* = 5.0 Hz, 1H), 8.03 (t, *J* = 7.0 Hz, 1H), 7.90 (d, *J* = 7.9 Hz, 1H), 7.78 (t, *J* = 8.0 Hz, 1H), 7.68-7.47 (m, 6H), 7.37 (s, 1H), 7.30 (d, *J* = 7.9 Hz, 1H), 6.91 (d, *J* = 7.8 Hz, 1H), 2.61 (t, *J* = 7.7 Hz, 2H), 1.74-1.57 (m, 2H), 1.48-1.34 (m, 2H), 1.16 (s, 42H), 0.95 (t, *J* = 7.3 Hz, 3H). ^{13}C NMR (75 MHz, CD_2Cl_2, DEPT 135): δ = 165.8 (C), 158.6 (C), 154.9 (C), 151.8 (CH), 147.2 (C), 144.9 (C), 142.6 (C), 139.3 (CH), 138.8 (CH), 135.4 (CH), 131.7 (CH), 129. 9 (C), 128.1 (CH), 124.9 (CH), 124.3 (CH), 123.9 (C), 123.2 (CH), 118.7 (CH), 117.9 (CH), 110.1 (C), 106.8 (C), 104.4 (C), 91.2 (C), 36.3 (CH_2), 34.0 (CH_2), 22.9 (CH_2), 18.9 (CH_3), 14.2 (CH_3), 11.8 (CH). HRMS MALDI: Calcd for $C_{50}H_{65}N_2PtSi_2$ $[M+H]^+$ 944.4331; found 944.4370.

Compound 3: A mixture 5/1 of benzene/ NEt_3 was added to a two neck RBF charged with **11** (87 mg, 0.108 mmol) and **8** (150 mg, 0.324 mmol) under Ar atmosphere. The mixture was stirred during 30 min. Then $Pd(PPh_3)_2Cl_2$ (8 mg, 0.007 mmol) and CuI (2 mg, 0.012 mmol) was introduced, and the reaction mixture was stirred for 3 h at room temperature. The mixture was then concentrated in vacuo and was purified by flash column chromatography on silica gel with hexane-CH_2Cl_2 (2:3). The obtained solid was sonicated with a hot mixture hexane-CH_2Cl_2 (4:1). The product was filtered off and washed with hot hexane to give **3** as a yellow solid (98 mg, 80%). ^{1}H NMR (300 MHz, CD_2Cl_2): δ = 8.65 (d, *J* = 5.7 Hz, 2H), 7.93 (d, *J* = 7.9 Hz, 2H), 7.84 (td, *J* = 7.7, 1.5 Hz, 2H), 7.65-7.55 (m, 4H), 7.54-7.48 (m, 3H), 7.32-7.23 (m, 2H), 7.17 (d, *J* = 8.2 Hz, 2H), 6.86 (td, *J* = 7.5, 1.2 Hz, 2H), 6.69 (td, *J* = 7.4, 1.3 Hz, 2H), 6.25 (d, *J* = 7.6 Hz, 2H), 1.55 (s, 6H), 1.14 (s, 42H). ^{13}C NMR (75 MHz, CD_2Cl_2, DEPT 135): δ = 183.9 (C), 168.7 (C), 148.6 (CH), 148.1 (C), 145.5 (C), 144.3 (C), 137.7 (CH), 134.9 (CH), 134.8 (CH), 133.6 (CH), 133.0 (CH), 132.3 (CH), 129.2 (CH), 124.6 (C), 124.37 (CH), 124.3 (C), 122.2 (CH), 121.2 (CH), 121.1 (C), 119.1 (CH), 115.7 (C), 105.6 (C), 92.8 (C), 90.9 (C), 87.9 (C), 29.5 (CH_3), 18.8 (CH_3), 11.73 (CH). HRMS ESI: Calcd for $C_{63}H_{71}IrN_2O_2Si_2$ $[M]^+$ 1136.4678; found 1136.4727.

Compound 13: Anhydrous CH_2Cl_2 (7 mL) was added to a Schlenk charged with **9** (200 mg, 0.348 mmol), **12** (89 mg, 0.290 mmol), Et_3N (1.2 mL) and CuI (14 mg, 0.078 mmol). The resulting mixture was bubbled with Ar for 3 min and stirred at room temperature for 24 h. The mixture was then concentrated in vacuo and purified by flash column chromatography on silica gel with hexane-CH_2Cl_2 (3:1) as eluent to give **13** (127 mg, 52%) as a yellow solid. ^{1}H NMR (300 MHz, $CDCl_3$): δ = 7.86 (s, 2H), 7.79 (t, *J* = 7.9 Hz, 1H), 7.69 (d, *J* = 7.7 Hz, 2H), 7.51 (s, 1H), 7.46 (d, *J* = 7.9 Hz, 2H), 7.37 (d, *J* = 8.0 Hz, 2H), 7.06 (d, *J* = 7.7 Hz, 2H), 3.08 (s, 1H), 2.65 (t, *J* = 7.7 Hz, 4H), 1.73-1.57 (m, 4H), 1.48-1.32 (m, 4H), 1.14 (s, 21H), 0.95 (t, *J* = 7.3 Hz, 6H). ^{13}C NMR (75 MHz, $CDCl_3$, DEPT 135): δ = 167.0 (C), 165.1 (C), 147.5 (C), 146.5 (C), 142.1 (CH), 136.8 (CH), 135.6 (CH), 135.1 (CH), 133.7 (CH), 127.6 (C), 126.9 (CH), 125.2 (CH), 124.0 (C), 122.5 (C), 116.0 (CH), 105.9 (C), 99.5 (C), 94.8 (C), 91.7 (C), 82.8 (C), 77.8 (CH), 36.2 (CH_2), 33.5 (CH_2), 22.6 (CH_2), 18.8 (CH_3), 14.1 (CH_3), 11.5 (CH). HRMS MALDI: Calcd for $C_{46}H_{53}AuNSi$ $[M+H]^+$: 844.3607; found 844.3609.

Compound 4: A Schlenk was charged with **10** (34 mg, 0.065 mmol), **13** (50 mg, 0.059 mmol), Et_3N (0.4 mL), CuI (2 mg, 0.010 mmol) and anhydrous CH_2Cl_2 (7 mL). Then Ar was bubbled into the mixture for 3 min and the mixture was stirred at 40 ºC for 48 h. The mixture was then concentrated in vacuo and was purified by flash column chromatography on neutral Al_2O_3 with hexane-CH_2Cl_2 (1:3). The obtained solid was sonicated with a hot mixture Hexane-CH_2Cl_2 (10:1). The compound was filtered off and washed with hot hexane to give **4** (60 mg, 77%) as an orange solid. ^{1}H RMN (300 MHz, CD_2Cl_2): δ = 9.17 (d, *J* = 5.2 Hz, 1H), 8.05 (t, *J* = 7.8 Hz, 1H), 7.92 (d, *J* = 7.9 Hz, 1H), 7.88-7.76 (m, 4H) , 7.74-7.66 (m, 2H), 7.64-7.45 (m, 7H), 7.41 (d, *J* = 8.0 Hz, 2H), 7.32 (d, *J* = 7.9 Hz, 1H), 7.08 (dd, *J* = 7.9, 1.7 Hz, 2H), 6.92 (d, *J* = 6.2 Hz, 1H), 2.73-2.56 (m, 6H), 1.75-1.57 (m, 6H), 1.48-1.30 (m, 6H), 1.01-0.85 (m, 9H). ^{13}C NMR (75 MHz, CD_2Cl_2, DEPT 135): δ = 167.2 (C), 165.8 (C), 165.2 (C), 158.5 (C), 154.9 (C), 151.8 (CH), 147.7 (C), 147.2 (C), 147.1 (C), 144.9 (C), 142.8 (C), 142.6 (CH), 139.2 (CH), 138.8 (CH), 137.0 (CH), 134.8 (CH), 134.0 (CH), 132.2 (CH), 129.8 (C), 128.0 (CH), 127.2 (C), 127.1(CH), 125.6 (CH), 124.9 (CH), 124.2 (CH), 123.7 (C), 123.2 (CH), 118.6 (CH), 117.9 (CH), 116.6 (CH), 109.3 (C), 107.4 (C), 104.8 (C), 100.6 (C), 93.5 (C) 9, 90.6 (C), 36.5 (CH_2), 36.4 (CH_2), 34.0 (CH_2), 33.9 (CH_2), 23.0 (CH_2), 22.9 (CH_2), 18.9 (CH_3), 14.3 (CH_3), 14.2 (CH_3), 11.8 (CH). HRMS MALDI: Calcd for $C_{66}H_{71}AuN_3PtSi$ $[M+H]^+$: 1325.4729; found 1325.4721.

Compound 14: A solution 1 M of tetra-*n*-butylammonium fluoride (0.2 mL, 0.185 mmol) in THF was added to a solution of **3** (70 mg, 0.062 mmol) in anhydrous THF (7 mL) under argon at -78 ºC. The mixture was stirred while was allowed to warm to room temperature (3 h). The solvent was evaporated and the residue was purified by flash chromatography on neutral Al_2O_3 with hexane-CH_2Cl_2 (2:3). Finally the obtained solid was washed with hot hexane afforded **14** (38 mg, 74%) as a yellow solid. ^{1}H NMR (300 MHz, CD_2Cl_2): δ = 8.65 (ddd, *J* = 5.8, 1.5, 0.8 Hz, 2H), 7.93 (d, *J* = 7.8 Hz, 2H), 7.88-7.79 (m, 2H), 7.66-7.58 (m, 4H), 7.58-7.49 (m, 3H), 7.28 (ddd, *J* = 7.3, 5.8, 1.5 Hz, 2H), 7.22-7.14 (m, 2H), 6.87 (td, *J* = 7.5, 1.2 Hz, 2H), 6.70 (td, *J* = 7.4, 1.4 Hz, 2H), 6.26 (dd, *J* = 7.6, 0.8 Hz, 2H), 3.20 (s, 2H), 1.56 (s, 6H). ^{13}C NMR (75 MHz, CD_2Cl_2, DEPT 135): δ = 183.9 (C), 168.7 (C), 148.6 (CH), 148.1 (C), 145.5 (C), 144.4 (C), 137.7 (CH), 135.5 (CH), 135.3 (CH), 133.6 (CH), 133.0 (CH), 132.4 (CH), 129.2 (CH), 124.7 (C), 124.4 (CH), 123.4 (C), 122.2 (CH), 121.2 (CH), 120.9 (C), 119.1 (CH), 115.7 (C), 91.3 (C), 87.6 (C), 82.0 (C), 78.9 (CH), 29.5 (CH3). HRMS MALDI: Calcd for $C_{45}H_{31}IrN_2O_2$ $[M]^+$ 824.2012; found 824.2025.

Compound 5: Anhydrous CH_2Cl_2 (5 mL) was added to Schlenk charged with **9** (30 mg, 0.052 mmol), **14** (73 mg, 0.088 mmol), Et_3N (0.5 mL) and CuI (3 mg, 0.014 mmol). The resulting mixture was bubbled with Ar for 3 min and then was stirred at 0 ºC for 3 h. The reaction mixture was then concentrated under reduced pressure. Purification by chromatography on aluminium oxide with CH_2Cl_2 as eluent, followed by crystallization by the slow diffusion of Et_2O in CH_2Cl_2 solution afforded **5** as a yellow solid (30 mg, 42%). ^{1}H NMR (300 MHz, CD_2Cl_2): δ = 8.66 (d, *J* = 5.7 Hz, 2H), 7.93 (d, *J* = 7.9 Hz, 2H), 7.89-7.79 (m, 5H), 7.75 (t, *J* = 1.5 Hz, 1H), 7.69 (t, *J* = 1.5 Hz, 1H), 7.64-7.49 (m, 7H), 7.42 (d, *J* = 8.0 Hz, 2H), 7.29 (ddd, *J* = 7.2, 5.8, 1.4 Hz, 2H), 7.18 (d, *J* = 8.1 Hz, 2H), 7.10 (dd, *J* = 7.9, 1.7 Hz, 2H), 6.86 (td, *J* = 7.5, 1.1 Hz, 2H), 6.70 (td, *J* = 7.4, 1.3 Hz, 2H), 6.26 (d, *J* = 7.6 Hz, 2H), 3.20 (s, 1H), 2.73-2.60 (m, 4H), 1.74-1.59 (m, 4H), 1.55 (s, 6H), 1.40 (m, 4H), 0.96 (t, *J* = 7.3 Hz, 6H). ^{13}C NMR (75 MHz, CD_2Cl_2, DEPT 135): δ = 183.9 (C), 168.7 (C), 167.0 (C), 165.2 (C), 148.6 (CH), 148.1 (C), 147.8 (C), 147.0 (C), 145.5 (C), 144.1 (C), 142.6 (CH), 137.7 (CH), 136.8 (CH), 135.3 (CH), 135.2 (CH), 133.5 (CH), 133.4 (CH), 132.9 (CH), 132.3 (CH), 129.2 (CH), 128.0 (C), 127.2 (CH), 125.6 (CH), 124.3 (CH), 124.2 (C), 122.9 (C), 122.2 (CH), 121.2 (C), 121.1 (CH), 119.0 (CH), 116.6 (CH), 115.7 (C), 99.6 (C), 95.5 (C), 88.3 (C), 82.7 (C), 78.2 (CH), 36.4 (CH_2), 33.9 (CH_2), 29.5 (CH_3), 22.9 (CH_2), 14.2 (CH_3). HRMS MALDI: Calcd for $C_{70}H_{57}AuIrN_3O_2$ $[M]^+$ 1361.3746; found 1361.3733.

Compound 6: To a two neck RBF charged with **14** (40 mg, 0.049 mmol) and **10** (13 mg, 0.024 mmol) and CuI (1 mg, 0.007 mmol) under Ar atmosphere were added anhydrous CH_2Cl_2 (5 mL) and NEt_3 (0.3 mL). The mixture was stirred during 3 h at room temperature. Then $Pd(PPh_3)_2Cl_2$ (3 mg, 0.004 mmol) and iodobenzene (138 mg, 0.900 mmol) was introduced, and the reaction mixture was stirred overnight at room temperature. The mixture was then concentrated under reduced pressure and was purified by flash column chromatography on neutral Al_2O_3 with CH_2Cl_2 as eluent. The obtained solid was sonicated with a hot mixture hexane-CH_2Cl_2 (4:1). Finally, the product was filtered off and washed with hot hexane to give **6** as an orange solid (22 mg, 65%). ^{1}H NMR (300 MHz, CD_2Cl_2): δ = 9.17 (d, *J* = 5.3 Hz, 1H), 8.66 (d, *J* = 5.2 Hz, 2H), 8.06 (t, *J* = 7.2 Hz, 1H), 7.98-7.09 (m, 27H), 6.93 (d, *J* = 6.9 Hz, 1H), 6.86 (t, *J* = 7.4 Hz, 2H), 6.69 (t, *J* = 7.3 Hz, 2H), 6.26 (d, *J* = 7.5 Hz, 2H), 2.71-2.57 (m, 2H), 1.74-1.60 (m, 2H), 1.57 (s, 6H), 1.51-1.34 (m, 2H), 1.02-0.90 (m, 3H). ^{13}C NMR (75 MHz, CD_2Cl_2): δ = 183.9, 168.7, 148.6, 148.1, 145.5, 139.2, 137.7, 133.6, 132.9, 132.3, 132.0, 132.0, 129.2, 128.9, 124.4, 122.2, 121.2, 119.1, 89.1, 36.4, 34.0, 29.6, 23.0, 14.3 (Not all the carbons are detected due to low solubility of the compound). HRMS MALDI: Calcd for $C_{71}H_{53}IrN_4NaO_2Pt$ $[M+Na]^+$ 1404.3347; found 1404.3347. Calcd for $C_{71}H_{53}IrN_4O_2Pt$ $[M]^+$ 1381.3450; found 1381.3400.

Compound 7: A Schlenk was charged with **5** (15 mg, 0.011 mmol), **10** (6 mg, 0.010 mmol), Et_3N (0.3 mL), CuI (6 mg, 0.029 mmol) and anhydrous CH_2Cl_2 (3 mL). Then Ar was bubbled into the mixture for 3 min. The mixture was stirred at 40 ºC for 48 hours and then concentrated in vacuo. The crude produced was purified by flash column chromatography on neutral Al_2O_3 with CH_2Cl_2 as eluent. The obtained solid was sonicated with a hot mixture of hexane-CH_2Cl_2 (4:1). The product was filtered off and washed with hot hexane to give **7** as an orange solid (10 mg, 49%). ^{1}H NMR (300 MHz, CD_2Cl_2): δ = 9.21 (d, *J* = 5.1 Hz, 1H), 8.66 (d, *J* = 5.5 Hz, 2H), 8.06 (t, *J* = 7.9 Hz, 1H), 7.99-7.77 (m, 9H), 7.78-7.69 (m, 2H), 7.66-7.46 (m, 11H), 7.42 (d, *J* = 8.0 Hz, 2H), 7.37-7.23 (m, 3H), 7.18 (d, *J* = 8.0 Hz, 2H), 7.09 (d, *J* = 7.9 Hz, 2H), 6.93 (d, *J* = 6.7 Hz, 1H), 6.86 (t, *J* = 7.4 Hz, 2H), 6.69 (t, *J* = 7.4 Hz, 2H), 6.26 (d, *J* = 7.4 Hz, 2H), 2.73-2.59 (m, 6H), 1.77-1.60 (m, 6H), 1.57 (s, 6H), 1.50 -1.32 (m, 6H), 1.02-0.87 (m, 9H). ^{13}C NMR (75 MHz, CD_2Cl_2): δ = 184.0, 168.7, 167.2, 166.0, 165.3, 158.6, 154.9, 151.9, 148.7, 148.2, 147.9, 147.3, 147.2, 145.5, 144.9, 143.8, 142.7, 142.7, 139.3, 137.7, 137.0, 133.6, 132.8, 132.33, 131.8, 129.8, 129.3, 129.2, 128.2, 127.3, 127.2, 125.6, 125.0, 124.4, 124.3, 123.5, 123.1, 122.2, 121.8, 121.1, 119.0, 118.7, 117.8, 116.6, 115.8, 100.7, 93.4, 89.6, 89.5, 36.5, 36.4, 34.0, 34.0, 29.5, 23.0, 23.0, 14.3, 14.2. (Not all the carbons are detected due to low solubility of the compound). HRMS MALDI: Calcd for $C_{90}H_{75}AuIrN_5O_2Pt$ $[M]^+$ 1842.4870; found 1842.4845.

Photophysical measurements. Absorption spectra were measured on a Biotek Instruments XS spectrometer, using quartz cuvettes of 1 cm path length. Steady-state luminescence spectra were measured using a Jobin Yvon FluoroMax-2 spectrofluorimeter, fitted with a red-sensitive Hamamatsu R928 photomultiplier tube; the spectra shown are corrected for the wavelength dependence of the detector, and the quoted emission maxima refer to the values after correction. Samples for emission measurements were contained within quartz cuvettes of 1 cm path length modified with appropriate glassware to allow connection to a high-vacuum line. Degassing was achieved via a minimum of three freeze-pump-thaw cycles whilst connected to the vacuum manifold; final vapour pressure at 77 K was $< 5 \times 10^{-2}$ mbar, as monitored using a Pirani gauge. Luminescence quantum yields were determined

using $[Ru(bpy)_3]Cl_2$ in degassed aqueous solution as the standard (Φ_{lum} = 0.042); estimated uncertainty in Φ_{lum} is ± 20% or better. The luminescence lifetimes of the complexes were measured by time-correlated single-photon counting, following excitation at 374.0 nm with an EPL-375 pulsed-diode laser. The emitted light was detected at 90° using a Peltier-cooled R928 PMT after passage through a monochromator. The estimated uncertainty in the quoted lifetimes is ± 10% or better. Low-temperature measurements were made using a home-built quartz dewar with the sample contained within 4 mm o.d. quartz tubes immersed in liquid nitrogen. For lifetimes exceeding 10 μs, a pulsed xenon flashlamp was used as the excitation source (an appropriate wavelength bring selected using a monochromator), in conjunction with the same R928 detector used in multichannel scaling mode.

Conclusions

In summary, we demonstrate how the 1,3,5-triethynylbenzene unit can be successfully used to link together three different metal centres using a modular synthetic approach. This linking core offers only minimal conjugation, such that the properties of the individual metal complexes are to a large extent retained in the supramolecular di- and tri-nuclear systems. For example, the absorption spectra of the multinuclear complexes in the longer-wavelength region, where the metal-based units absorb, match well with the spectra simulated by addition of the spectra of the mononuclear metal complexes.

In the multinuclear complexes containing both Ir(III) and Pt(II) units, emission attributable to both moieties is observed, but the intensity and lifetime of the higher-energy Ir(III)-based emission are greatly reduced compared to the mononuclear iridium complex, attributable to energy transfer from the Ir unit to the Pt unit. The overlap of the emission spectrum of the former with the absorption spectrum of the latter is quite limited, and the calculated Förster rate constant is not sufficient to fully account for the the experimentally observed energy transfer rate, suggesting a significant through-bond Dexter component to the process. No detectable Au-based emission is observed at room temperature in the gold-containing multinuclear complexes **4**, **5** and **7**, indicative of energy transfer from the Au unit to the Ir and Pt units, as expected on the basis of the order of the excited state energies of the individual components.

The simultaneous emission from both the Ir and Pt units in **6** and in **7** leads to broad-band emission covering much of the visible region of the spectrum, and CIE coordinates of x = 0.50, y = 0.49 for **7**. It is clear, however, that in order to obtain an efficient *white* light emitter, the molecular design would need to be modified in such a way as to (i) further slow the rate of Ir→Pt energy transfer, and (ii) incorporate a more efficient blue emitter than the N^C^N-coordinated Au unit, whose quantum yield is very low.

Acknowledgements

DJC thanks the Ministerio de Ciencia e Innovación (CTQ2010-15927), and the CAM (AVANCAT and CCG06-UAM/PPQ-0132) for financial support; as well as the UAM for a fellowship to RM-R. JAGW thanks EPSRC (grant reference EP/G06928X/1) for support.

Notes and references

[a] Department of Organic Chemistry, Facultad de Ciencias, Universidad Autónoma de Madrid, Cantoblanco, 28049-Madrid, Spain.

[b] Department of Chemistry, Durham University, Durham, DH1 3LE, United Kingdom.

Electronic Supplementary Information (ESI) available: [details of any supplementary information available should be included here]. See DOI: 10.1039/b000000x/

1 H. Yersin, *Highly Efficient OLEDs with Phosphorescent Materials*, Wiley-VCH, Weinheim, 2008.

2 C. Adachi, M. A. Baldo, M. E. Thompson, S. R. Forrest, *J. Appl. Phys.*, 2001, **90**, 5048.

3 J. Kalinowski, *Organic light-emitting diodes: principles, characteristics, and processes*, CRC Press, New York, 2005.

4 L. F. Gildea, J. A. G. Williams, *Organic light-emitting diodes: Materials, devices and applications*, Woodhead, Cambridge, 2013.

5 P. K. M. Siu, S.-W. LaiLu, N. Zhu, C.-M. Che, *Eur. J. Inorg. Chem.*, 2003, 2749.

6 W. Tang, X. Lu, K. Wong, V. Yam, *J. Mater. Chem.*, 2005, **15**, 2714.

7 N. C. Fletcher, M. C. Lagunas, *Top. Organomet. Chem.*, 2010, 38, 143; Q. Zhao, F. Li, C. Huang, *Chem. Soc. Rev.*, 2010, **39**, 3007.

8 V. Fernandez-Moreira, F. L. Thorp-Greenwood, M. P. Coogan, *Chem. Commun.*, 2010, **46**, 186; K. K. W. Lo, K. Y. Zhang, *RSC Adv.*, 2012, **32**, 12069; Q. Zhao, C. Huang, F. Li, *Chem. Soc. Rev.*, 2011, **40**, 2508; E. Baggaley, J. A. Weinstein, J. A. G. Williams, *Coord. Chem. Rev.*, 2012, **256**, 1762; D. Septiadi, A. Aliprandi, M. Mauro, L. De Cola, *RSC Adv.*, 2014, **4**, 25709; M. Mauro, A. Aliprandi, D. Septiadi, N. S. Kehr, L. De Cola, *Chem. Soc. Rev.*, 2014, **43**, 4144; E. Baggaley, S. W. Botchway, J. W. Haycock, H. Morris, I. V. Sazanovich, J. A. G. Williams, J. A. Weinstein. *Chem. Sci.*, 2014, **5**, 879.

9 V. Guerchais, L. Ordronneau, H. Le Bozec, *Coord. Chem. Rev.*, 2010, **254**, 2533; S. Di Bella, C. Dragonetti, M. Pizzotti, D. Roberto, F. Tessore, R. Ugo, *Top. Organomet. Chem*., 2010, **28**, 1; M. G. Humphrey, M. P. Cifuentes, M. Samoc, *Top. Organomet. Chem.*, 2010, **28**, 57.

10 V. Aubert, L. Ordronneau, M. Escadeillas, J. A. G. Williams, A. Boucekkine, E. Coulaud, C. Dragonetti, S. Righetto, D. Roberto, R. Ugo, A. Valore, A. Singh, J. Zyss, I. Ledoux-Rak, H. Le Bozec, V. Guerchais, *Inorg. Chem.*, 2011, **50**, 5027; J. Boixel, V. Guerchais, H. Le Bozec, D. Jacquemin, A. Amar, A. Boucekkine, A. Colombo, C. Dragonetti, D. Marinotto, D. Roberto, S. Righetto, R. De Angelis, *J. Am. Chem. Soc*., 2014, **136**, 5367; C. Dragonetti, A. Colombo, D. Marinotto, S. Righetto, D. Roberto, A. Valore, M. Escadeillas, V. Guerchais, H. Le Bozec, A. Boucekkine, C. Latouche *J. Organomet. Chem.*, 2014, **751**, 568; M. Zaarour, A. Singh, C. Latouche, J. A. G. Williams, I. Ledoux-Rak, J. Zyss, A. Boucekkine, H. Le Bozec, V. Guerchais, C. Dragonetti, A. Colombo, D. Roberto, A. Valore, *Inorg. Chem.*, 2013, **52**, 7987; A. Colombo, C. Dragonetti, D. Marinotto, S. Righetto, D. Roberto, S. Tavazzi, M. Escadeillas, V. Guerchais, H. Le Bozec, A. Boucekkine, C. Latouche, *Organometallics*, 2013, **32**, 3890; E. Rossi, A. Colombo, S. Righetto, D. Roberto, R. Ugo, A.

Valore, J. A. G. Williams, M. G. Lobello, F. De Angelis, S. Fantacci, I. Ledoux-Rak, A. Singh, J. Zyss, *Chem. Eur J.*, 2013, **19**, 9875; A. Valore, A. Colombo, C. Dragonetti, S. Righetto, D. Roberto, R. Ugo, F. De Angelis, S. Fantacci, *Chem. Commun*., 2010, **46**, 2414.

11 H. Yersin, A. F. Rausch, R. Czerwieniec, T. Hofbeck, T. Fischer, *Coord. Chem. Rev.*, 2011, **255**, 2622.

12 M. A. Baldo, D. F. O'Brien, Y. You, A. Shoustikov, S. Sibley, M. E. Thompson, S. R. Forrest, *Nature*, 1998, **395**, 151.

13 S. W. Botchway, M. Charnley, J. W. Haycock, A. W. Parker, D. L. Rochester, J. A. Weinstein, J. A. G. Williams, *Proc. Natl. Acad. Sci. USA,* 2008, **105**, 16071; L. Murphy, A. Congreve, L.-O. Palsson, J. A. G. Williams, *Chem. Commun.*, 2010, **46**, 8743; E. Baggaley, S. W. Botchway, J. W.; Haycock, H. Morris, I. V. Sazanovich, J. A. G. Williams, J. A. Weinstein, *Chem. Sci.*, 2014, **5**, 879.

14 Y. H. Son, M. J. Park, Y. J. Kim, J. H. Yang, J. S. Park, J. H. Kwon, *Org. Electron.*, 2013, **14**, 1183.

15 S. Tasch, E. J. W. List, O. Ekstrom, W. Graupner, G. Leising, P. Schlichting, U. Rohr, Y. Geerts, U. Scherf, K. Mullen, *Appl. Phys. Lett.*, 1997, **71**, 2883; P.-I. Shih, C.-F. Shu, Y.-L. Tung, Y. Chi, *Appl. Phys. Lett.*, 2006, **88**, 251110; B. W. D'Andrade, R. J. Holmes, S. R. Forrest, *Adv. Mater.,* 2004, **16**, 624; J. Kido, H. Shionoya, K. Nagai, *Appl. Phys. Lett.*, 1995, **67**, 2281; M. Granström, O. Inganäs, *Appl. Phys. Lett.***,** 1995, **68**, 147; J.-H. Jou, M.-C. Sun, H.-H. Chou, C.-H. Li, *Appl. Phys. Lett.*, 2005, **87**, 043508.

16 V. Adamovich, J. Brooks, A. Tamayo, A. M. Alexander, P. I. Djurovich, B. W D'Andrade, C. Adachi, S. R. Forrest, M. E. Thompson, *New J. Chem.*, 2002, **26**, 1171; B. W. D'Andrade, J. Brooks, V. Adamovich, M. E. Thompson. S. R. Forrest, *Adv. Mater.*, 2002, **14**, 1032; M. Cocchi, J. Kalinowski, L. Murphy, J. A. G. Williams, V. Fattori, *Org. Electron,* 2010, **11**, 388; L. Murphy, P. Brulatti, V. Fattori, M. Cocchi, J. A. G. Williams, *Chem. Commun*., 2012, **48**, 5817.

17 L. Flamigni, A. Barbieri, C. Sabatini, B. Ventura, F. Barigelletti, *Top. Curr. Chem*., 2007, **281**, 143; J. A. G. Williams, *Top. Curr. Chem.*, 2007, **281**, 205; K. P. Balashev, M. V. Puzyk, V. S. Kotlyar, M. V. Kulikova, *Coord. Chem. Rev.*, 1997, **159**, 109; J. Brooks, Y. Babayan, S. Lamansky, P. I. Djurovich, I. Tsyba, R. Bau, M. E. Thompson, *Inorg. Chem*., 2002, **41**, 3055 ; B. L. Yin, F. Niemeyer, J. A. G. Williams, J. Jiang, A. Boucekkine, L. Toupet, H. Le Bozec, V. Guerchais, *Inorg. Chem*., 2006, **45**, 8584; F. Niedermair, O. Kwon, K. Zojer, S. Kappaun, G. Trimmel, K. Mereiter, C. Slugovc, *Dalton Trans*., 2008, 4006; M. Ghedini, T. Pugliese, M. La Deda, N. Godbert, I. Aiello, M. Amati, S. Belviso, F. Lelj, G. Accorsi, F. Barigelletti, *Dalton Trans*., 2008, 4303; S.-Y. Chang, Cheng, Y Chi, Y.-C. Lin, C.-M. Jiang, G.-H. Lee, P.-T. Chou, *Dalton Trans*., 2008, 6901; J. Liu, C.-J. Yang, Q.-Y. Cao, M. Xu, J. Wang, H.-N. Peng, W.-F. Tan, X.-X. Lue, X.-C. Gao, *Inorg. Chim. Acta*, 2009, **362**, 575; A. Santoro, A. C. Whitwood, J. A. G. Williams, V. N. Kozhevnikov, D. W. Bruce, *Chem. Mater*., 2009, **21**, 3871; G. Zhou, Q. Wang, C.-L. Ho, W.-Y. Wong, D. Ma, L. Wang, *Chem. Commun*., 2009, 3574; K. Feng, C. Zuniga, Y.-D. Zhang, D. Kim, S. Barlow, S. R. Marder, J. L. Brédas, M. Weck, *Macromolecules*, 2009, **42**, 6855; G. J. Zhou, Q. Wang, X. Z. Wang, C. L. Ho, W. Y. Wong, D. G. Ma, L. X. Wang, Z. Y. Lin, *J. Mater. Chem*., 2010, **20**, 7472; D. A. K. Vezzu, J. C. Deaton, J. S. Jones, L. C. Bartolotti, F. Harris, A. P. Marchetti, M. Kondakova, R. D. Pike, S. Huo, *Inorg. Chem*., 2010, **49**, 5107; W. H. Wu, W. T. Wu, S. M. Ji, H. M. Guo, P. Song, K. L. Han, L. N. Chi, J. Y. Shao, J. Z. Zhao, *J. Mater. Chem*., 2010, **20**, 9775; J.C.-H. Chan, W. H. Lam, H.-L. Wong, N. Y. Zhu, W.-T. Wong. V.W.-W. Yam, *J. Am. Chem. Soc.*, 2011, **133**, 12690; C. Bronner, O. S. Wenger, *Dalton Trans*., 2011, **40**, 12409; S. Fuertes, S. K. Brayshaw, P. R. Raithby, S. Schiffers, M. R. Warren, *Organometallics*, 2012, **31**, 105; E. Turner, N. Bakken, J. Li, *Inorg. Chem*., 2013, **52**, 7344; C. F. Harris, D. A. P. Vezzu, L. Bartolotti, P. D. Boyle, S. Huo, *Inorg. Chem*., 2013, **52**, 11711.

18 M. A. Baldo, M. E. Thompson, S. R. Forrest, *Nature*, 2000, **403**, 750; A. Tsuboyama, H. Iwawaki, M. Furugori, T. Mukaide, J. Kamatani, S. Igawa, T. Moriyama, S. Miura, T. Takiguchi, S. Okada, M. Hoshino, K. Ueno, *J. Am. Chem. Soc*., 2003, **125**, 12971; V. A. Montes, C. Perez-Bolívar, N. Agarwal, J. Shinar, P. Anzenbacher, *J. Am. Chem. Soc*., 2006, **128**, 12436.

19 S.-W. Lai, M. C.-W. Chan, T.-C. Cheung, S.-M. Peng, C.-M. Che, *Inorg. Chem*., 1999, **38**, 4046; W. Lu, B.-X. Mi, M. C. W. Chan, Z. Hui, C.-M. Che, N. Zhu, S.-T. Lee, *J. Am. Chem. Soc*., 2004, **126**, 4958; W. Lu, M. C.-W.; Chan, N. Zhu, C.-M. Che, C. Li, Z. Hui, *J. Am. Chem. Soc*., 2004, **126**, 7639; S. Develay, O. Blackburn, A. L. Thompson, J. A. G. Williams, *Inorg. Chem.*, 2008, **47**, 11129; J. A. G. Williams, *Chem. Soc. Rev*., 2009, **38**, 1783.

20 F. Nisic, A. Colombo, C. Dragonetti, D. Roberto, A. Valore, J M. Malicka, M. Cocchi, G. R. Freeman, J. A. G. Williams*, J. Mater. Chem. C*, 2014, **2**, 1791; W. Mróz, C. Botta, U. Giovanella, E. Rossi, A. Colombo, C. Dragonetti, D. Roberto, R. Ugo, A. Valore, J. A. G. Williams, *J. Mater. Chem*., 2011, **21**, 8653; E. Rossi, A. Colombo, C. Dragonetti, D. Roberto, R. Ugo, A. Valore, L. Falciola, P. Brulatti, M. Cocchi and J. A. G. Williams, *J. Mater. Chem*., 2012, **22**, 10650.

21 V. W.-W. Yam, E. C.-C. Cheng, *Chem. Soc. Rev.*, 2008, **37**, 1806; C. Bronner, O. S. Wenger, *Dalton Trans.*, 2011, **40**, 12409.

22 V. W.-W. Yam, K. M.-C. Wong, L.-L. Hung, N. Zhu, *Angew. Chem. Int. Ed*., 2005, **44**, 3107; V. K.-M. Au, K. M.-C. Wong, N. Zhu, V. W.-W. Yam, *J. Am. Chem. Soc*., 2009, **131**, 9076; J. J. Yan, A. L.-F. Chow, C.-H. Leung, R. W.-Y. Sun, D.-L. Ma, C.-M. Che, *Chem. Commun*., 2010, **46**, 3893; V. K.-M. Au, K. M.-C. Wong, N. Zhu, V. W.-W. Yam, *Chem. Eur. J*., 2011, **17**, 130; A. Herbst, C. Bronner, P. Dechambenoit, O. S. Wenger, *Organometallics*, 2013, **32**, 1807.

23 S. Develay, J. A. G. Williams, *Dalton Trans*., 2008, 4562.

24 R. Muñoz-Rodríguez, E. Buñuel, J. A. G. Williams, D. J. Cárdenas, *Chem. Commun*., 2012, **48**, 5980.

25 K. J. Arm, J. A. G. Williams, *Chem. Commun*., 2005, 230; C. Sabatini, A. Barbieri, F. Barigelletti, K. J. Arm, J. A. G. Williams, *Photochem. Photobiol. Sci.*, 2007, **6**, 397.

26 J. H. Vandieman, R. Hage, J. G. Haasnoot, H. E. B. Lempers, J. Reedijk, J. G. Vos, L. De Cola, F. Barigelletti, V. Balzani, *Inorg. Chem.*, 1992, **31**, 3518; I. Ortmans, P. Didier, A. Kirsch-Demesmaeker, *Inorg. Chem.*, 1995, **34**, 3695.

27 T. Bura, M. P. Gullo, B. Ventura, A. Barbieri, R. Ziessel, *Inorg. Chem.*, 2013, **52**, 8653; B. Ventura, A. Barbieri, A. Degli Esposti, J. B. Seneclauze, R. Ziessel, *Inorg. Chem.*, 2012, **51**, 2832; B. Ventura, A. Barbieri, F. Barigelletti, S. Diring, R. Ziessel, *Inorg. Chem.*, 2010, **49**, 8333; B. Ventura, A. Barbieri, F. Barigelletti, J. B. Seneclauze, P. Retailleau, R. Ziessel, *Inorg. Chem*., 2008, **47**, 7048; A. Barbieri, B. Ventura and R. Ziessel, *Coord. Chem. Rev.*, 2012, **256**, 1732; M. P. Gullo, J. B. Seneclauze, B. Ventura, A. Barbieri, R. Ziessel, *Dalton Trans*., 2013, **42**, 16818.

28 V: N. Kozhevnikov, M. C. Durrant, J. A. G. Williams, *Inorg. Chem.,* 2011, **50**, 6304.

29 K. L. Chandra, S. Zhang, C. B. Gorman, *Tetrahedron*, 2007, **63**, 7120.

30 F. Spaenig, J.-H. Olivier, V. Prusakova, P. Retailleau, R. Ziessel, F. N. Castellano, *Inorg. Chem.*, 2011, **50**, 10859.

31 K. Onitsuka, M. Fujimoto, O. Masanori, N. Ohshiro, S. Takahashi, *Angew. Chem. Int. Ed.,* 1999, **38**, 689; K. Onitsuka, M. Fujimoto, H. Kitajima, N. Ohshiro, F. Takei, S. Takahashi, *Chem. Eur. J.*, 2004, **10**, 6433; V. W.-W. Yam, Vivian, L. Zhang, C.-H. Tao, K. M.-C. Wong, K.-K. Cheung, *J. Chem. Soc., Dalton Trans*., 2001, 1111; K. Cantin, A. Lafleur-Lambert, P. Dufour, J.-F. Morin, *Eur. J. Org. Chem*., 2012, 5335; M. Juricek, M. Felici, P. Contreras-Carballada, J. Lauko, Jan; S. R. Bou, P. H. J. Kouwer, A. M. Brouwer, A. E. Rowan, *J. Mater. Chem*., 2011, **21**, 2104**.**

32 V. W.-W. Yam, K. M.-C. Wong, L.-L. Hung, N. Zhu, *Angew. Chem., Int. Ed.*, 2005, **44**, 3107.

33 S. Lamansky, P. I. Djurovich, D. Murphy, A.-R. Feras, H.-E. Lee, C. Adachi, P. E. Burrows, S. R. Forrest, M. E. Thompson, *J. Am. Chem. Soc*., 2001, **123**, 4304.

34 The approach used follows the standard treatment, as described in, for example: J. R. Lakowicz, *Principles of Fluorescence Spectroscopy*, 3rd edition, Chapter 13, Springer, New York, 2006.

Journal Name RSCPublishing

ARTICLE

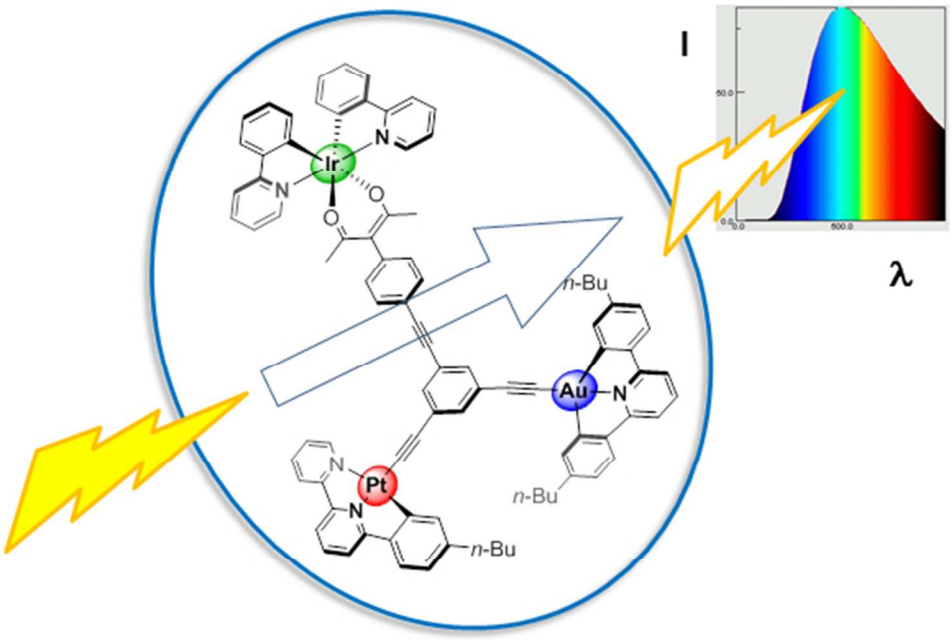

161x109mm (96 x 96 DPI)